Effect of CO_2 inhibition on biogenic isoprene emission: implications for air quality under 2000-to-2050 changes in climate, vegetation and land use

A.P.K. Tai, L.J. Mickley, S. Wu, C.L. Heald

Supplementary Materials (SM)

S1. Detailed model description

We provide here additional details for the GEOS-Chem chemical transport model. We refer to *Wu et al.* [2012] for details of the LPJ dynamic global vegetation model.

Anthropogenic emissions of ozone precursors (e.g., NO_x) are described by *Zhang et al.* [2011]. In GEOS-Chem, the land cover affects ozone production through dry deposition, soil nitrogen oxide (NO_x) emission, and biogenic volatile organic compound (VOC) emissions. Dry deposition velocity depends on vegetation type and generally increases with leaf area index (LAI). Soil NO_x emission is computed as a function of vegetation type, temperature, precipitation history, and fertilizer usage. Generally, grasslands and croplands emit more soil NO_x than forests. Here we treat isoprene nitrate as a terminal sink for NO_x without recycling, which represents the strongest sensitivity of ozone production to isoprene emission in NO_x-limited environments. Secondary organic aerosol (SOA) formation is based on the reversible gas-aerosol partitioning of VOC oxidation products [*Chung and Seinfeld*, 2002] with precursors including isoprene, terpenes, alcohols, and aromatic hydrocarbons.

The MEGAN v2.1 scheme [*Guenther et al.*, 2012] models isoprene emission (E_{isop}) as:

$$E_{\text{isop}} = \left(\sum_{j=1}^{5} \varepsilon_j \chi_j\right) \gamma_T \gamma_{\text{SM}} \gamma_{\text{age}} \gamma_{\text{CE}} \qquad (1)$$

but with the original 15 plant function types (PFTs) in LPJ re-categorized into five major PFTs as used in GEOS-Chem, where ε_j is the emission factor at baseline conditions and χ_j is the fractional coverage for each PFT j. The dimensionless activity factor γ describes any deviation from baseline conditions due to the effects of temperature (T), soil moisture (SM) (assumed to be unity here), leaf age, and canopy environment (CE) (including effects of light and LAI). In general, broadleaf forests are the most isoprene-emitting vegetation type, whereas grasslands and croplands emit the least isoprene.

References:

Chung, S. H., and J. H. Seinfeld (2002), Global distribution and climate forcing of carbonaceous aerosols, *J. Geophys. Res.-Atmos.*, *107*(D19), 4407, doi:10.1029/2001jd001397.

Guenther, A., X. Jiang, C. L. Heald, T. Sakulyanontvittaya, T. Duhl, L. K. Emmons, and X. Wang (2012), The Model of Emissions of Gases and Aerosols from Nature version 2.1 (MEGAN2.1): an extended and updated framework for modeling biogenic emissions, *Geosci Model Dev*, *5*(6), 1471-1492, doi:10.5194/Gmd-5-1471-2012.

Wu, S., L. J. Mickley, J. O. Kaplan, and D. J. Jacob (2012), Impacts of changes in land use and land cover on atmospheric chemistry and air quality over the 21st century, *Atmos. Chem. Phys.*, *12*(3), 1597-1609, doi:10.5194/Acp-12-1597-2012.

Zhang, L., D. J. Jacob, N. V. Downey, D. A. Wood, D. Blewitt, C. C. Carouge, A. van Donkelaar, D. B. A. Jones, L. T. Murray, and Y. X. Wang (2011), Improved estimate of the policy-relevant background ozone in the United States using the GEOS-Chem global model with 1/2 degrees x 2/3 degrees horizontal resolution over North America, *Atmos. Environ.*, *45*(37), 6769-6776, doi:10.1016/J.Atmosenv.2011.07.054.

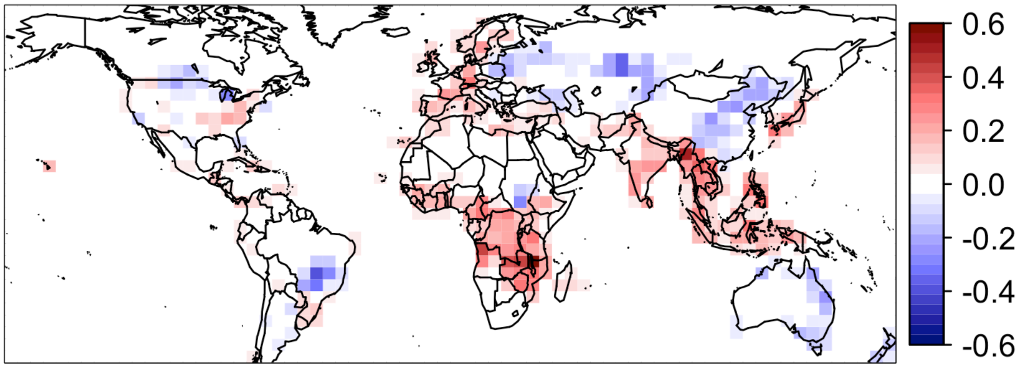

S2. Projected 2000-to-2050 changes in cropland fraction consistent with the IPCC A1B scenario [*IMAGE-Team*, 2001].

Reference:

IMAGE-Team (2001), The IMAGE 2.2 implementation of the SRES scenarios: A comprehensive analysis of emissions, climate change and impacts in the 21st century, RIVM CD-ROM publication 481508018, National Institute for Public Health and the Environment, Bilthoven, The Netherlands.

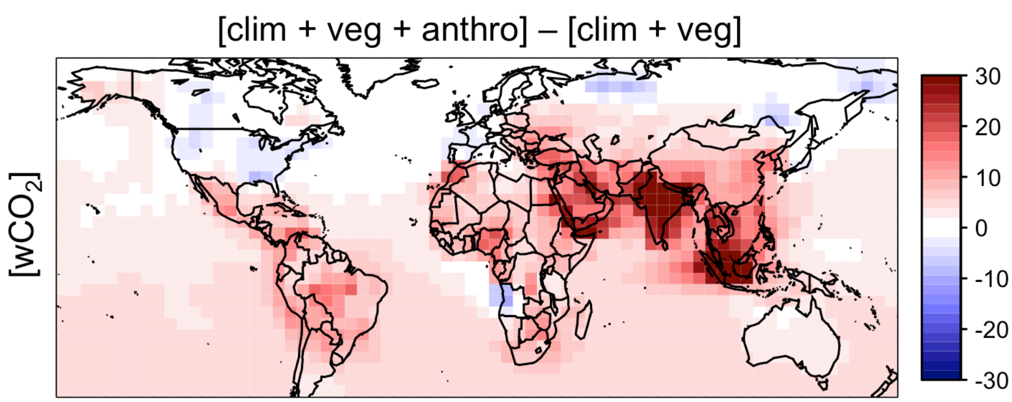

S3. Projected 2000-to-2050 changes in surface ozone concentration in response to changes in anthropogenic emissions of ozone and PM precursors with CO_2 inhibition of isoprene emission ([wCO_2]), as represented by the difference between the [clim + veg] and [clim + veg + anthro] scenarios. Values are mean boreal summer (JJA) daily maximum 8-h averages.

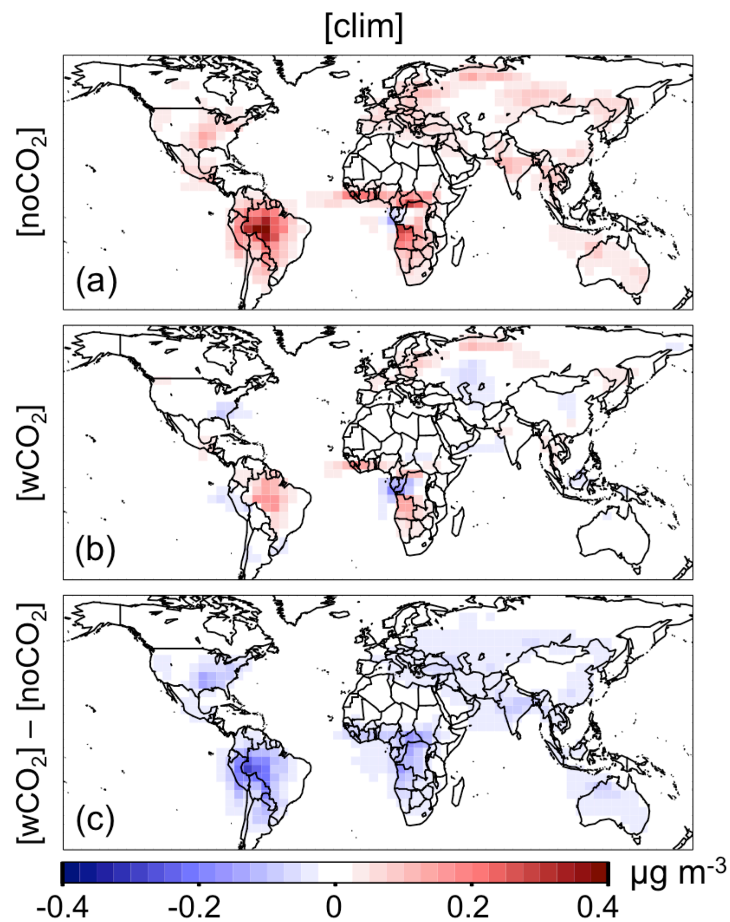

S4. Projected 2000-to-2050 changes in surface SOA concentration in response to climate change (a) without ([noCO_2]) and (b) with ([wCO_2]) the CO_2 inhibition of isoprene emission. (c) The difference between the [wCO_2] and [noCO_2] cases. Results are for the [clim] simulations that consider only the effects of projected 2050 climate change with constant, present-day land cover. Values are annual means.

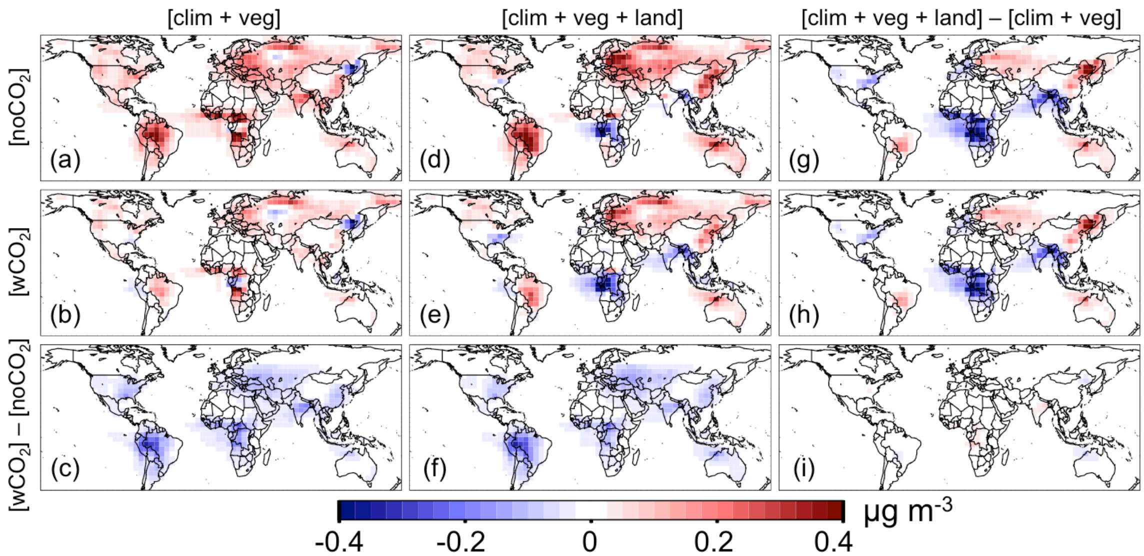

S5. Projected 2000-to-2050 changes in surface SOA concentration in response to changes in climate, natural vegetation, and anthropogenic land use, without ([noCO_2]) and with ([wCO_2]) CO_2 inhibition of isoprene emission. Results are for (a)-(c) the [clim + veg] simulations that consider changes in climate and natural vegetation, and (d)-(f) the [clim + veg + land] simulations that also include projected changes in anthropogenic land use. Panels (c), (f) and (i) show the differences between the [wCO_2] and [noCO_2] cases. Panels (g)-(i) represent the impact of land use change alone as represented by the difference between [clim + veg] and [clim + veg + land]. Values are annual means.

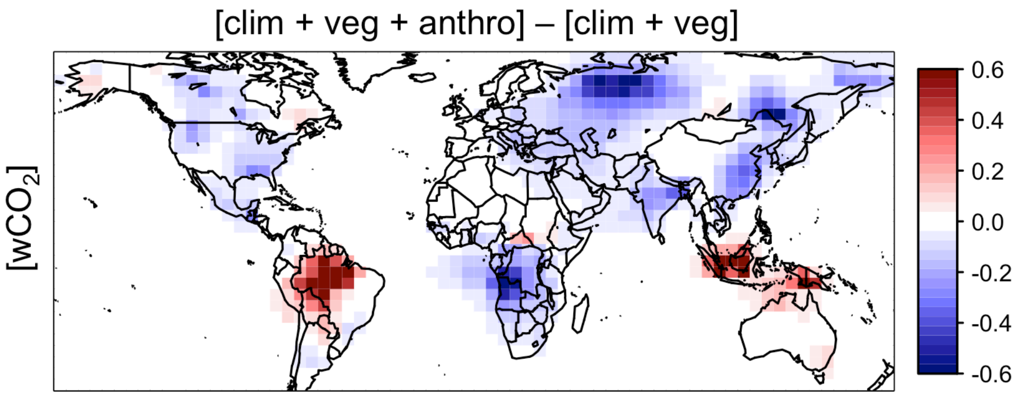

S6. Projected 2000-to-2050 changes in surface secondary organic aerosol (SOA) in response to changes in anthropogenic emissions of ozone and PM precursors with CO_2 inhibition of isoprene emission ([wCO_2]), as represented by the difference between the [clim + veg] and [clim + veg + anthro] scenarios. Values are annual means. The impact of land use change on SOA as shown in S5(h) is comparable in magnitude with that of changing anthropogenic emissions, which influence SOA mainly through affecting preexisting primary organic aerosol onto which secondary organic gases condense.